PERFORMANCE OF THE RENEWED L-BAND LINAC AND RECENT PROGRESS OF DEVELOPMENT OF FEL AND SASE AT OSAKA UNIVERSITY

G. Isoyama#, R. Kato, S. Kashiwagi, T. Igo, Y. Kon, T. Yamamoto, S. Suemine,
Institute of Scientific and Industrial Research, Osaka University
8-1 Mihogaoka, Ibaraki, Osaka 567-0047, Japan.

Abstract

We have evaluated performance of the L-band linac at ISIR, Osaka University in view of stability after the large-scale remodeling followed by commissioning made in 2002-2004. The beam intensity accelerated with the linac is measured for longer than one hour at some locations along the linac and beam lines, and intensity fluctuations are derived. The beam intensity fluctuation in one of the operation modes, most favorable for stability, is 0.25 % at the exit of the linac, which is one tenth of a value before remodeling. Recent progress of FEL and SASE experiments based on the renewed L-band linac is briefly introduced, including the development of a strong focus wiggler and SASE experiments in the far-infrared region using the new wiggler.

INTRODUCTION

The 40 MeV, L-band electron linac at the Institute of Scientific and Industrial Research (ISIR), Osaka University is used for various studies on advanced beam sciences, including development of a far-infrared FEL and basic study of SASE in the wavelength region. The linac was constructed in 1975-1978 and largely remodeled in 2002-2004 for higher operational stability and reproducibility. We reported an outline of the upgrade at APAC 04 [1], when the commissioning of the linac was still going on. The linac can be operated various operation modes such as the transient mode, in which an electron pulse consists of approximately 10 electron bunches separated by the interval of 0.77 ns and hence they are 8 ns long, the single bunch mode, in which a single electron bunch with the time duration of approximately 20 ps is accelerated, and the multi-bunch mode for FEL, in which an electron pulse is 8 μs long but intervals between bunches are 9.2 ns. We continued the commissioning of the linac progressively and we have completed the first two operation modes. Experiments have been resumed using the linac operated in the two modes.

In this paper we will report preliminary results of performance of the renewed linac and recent activities related to FEL and SASE experiments.

PERFORMANCE OF LINAC

A schematic drawing of the L-band linac and its beam lines are shown in Fig. 1. Almost all the power supplies for the linac, including the pulse modulator for the klystron, are replaced with new ones or refurbished completely in order to make stability of the linac and reproducibility of operation high. The main parameters of the linac before and after the remodelling are listed in Table 1. As can be seen in the Table 1, surface performance does not change by the upgrade. The maximum energy, for example, increases slightly from 38 to 40 MeV, but the peak current or the maximum charge

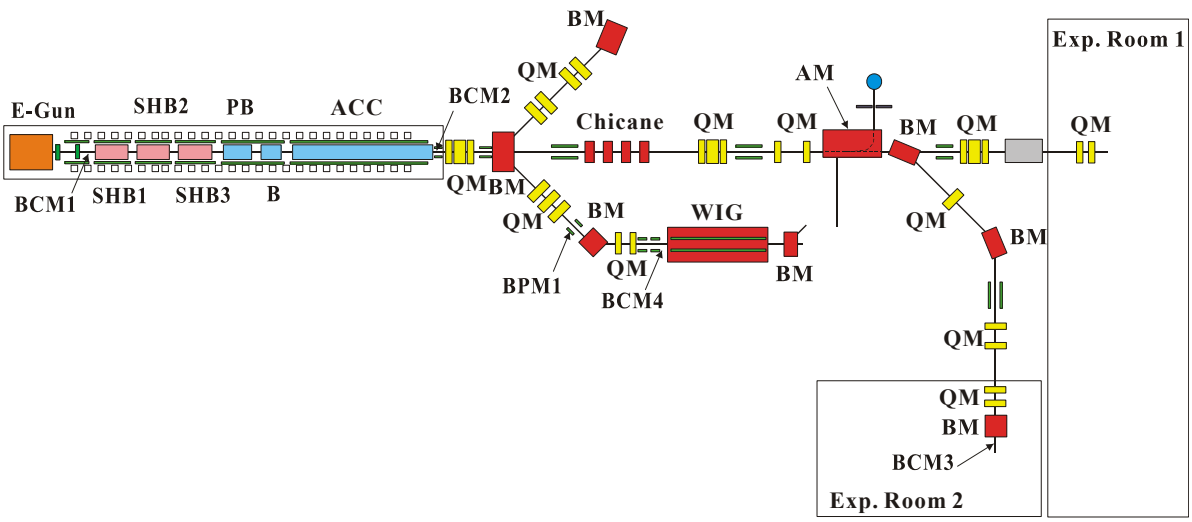

Figure 1: Schematic drawing of the L-band linac and its beam lines. E-Gun: electron gun, SHB: sub-harmonic buncher, PB: pre-buncher, B: buncher, ACC: accelerating tube, BM: bending magnet, QM: quadrupole magnet, AM: analyser magnet, WIG: wiggler, BCM: beam current monitor, BPM: beam position monitor.

#isoyama@sanken.osaka-u.ac.jp

per bunch is same in each operation mode. Observable changes are that the number of klystrons is reduced from two to one, which is favourable in view of stability, and that the maximum pulse width is extended twice from 4 to 8 μs for FEL.

Table 1: Main parameters of the L-band linac

	Before remodeling	After remodeling
Acc. frequency	1.3 GHz	
Sub-harmonic bunchers	108MHz × 2 216MHz × 1	
Accelerating structures	Prebuncher × 1 Buncher × 1 Accelerating tube × 1	
Injector	Thermionic gun (DC 100kV)	
Peak Current or Maximum charge per bunch	1.9 A (Steady mode) 30.6 A (Transient mode) 91 nC (Single-bunch mode) 1.9 A (Multibunch mode)	
Max. energy	38 MeV	40 MeV
Pulse width	20 ps - 4 μs	20 ps - 8 μs
Max. repetition	720 pps	60 pps
No of Klystrons	2 (5 MW+20 MW)	1 (30 MW)
Total length	10.5 m	

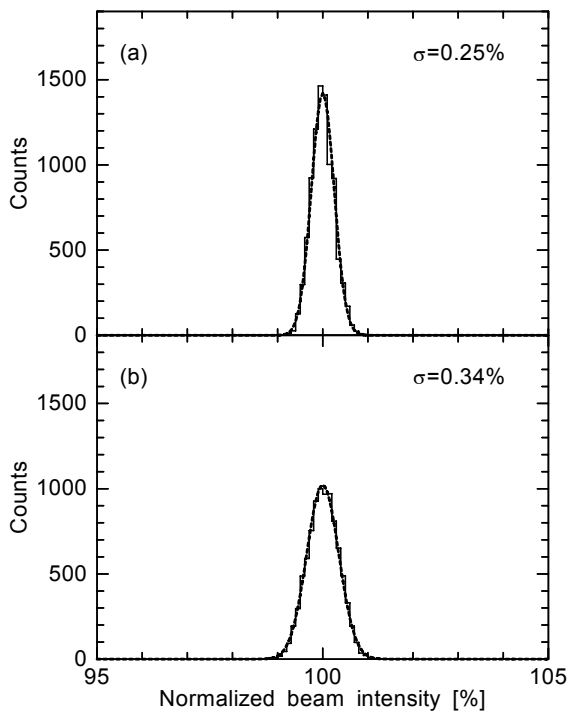

Figure 2: Histograms of the normalized beam intensities in the transient mode measured with (a) BCM2 at the exit of the linac and (b) BCM3 at the beam port in the 2nd experimental room. The dashed lines show least square fits of Gaussian functions.

In order to evaluate the performance in stability, we have measured the beam intensity in the transient mode for more than one hour using the beam current monitors at the exit of the linac and at the beam port in the second measurement room denoted respectively by BCM2 and BCM3 in Fig. 1. Since only the single RF source is used in the transient mode, it should be the most stable operation mode. Fig. 2 shows histogram of the relative beam intensities measured at the exit of the linac and at the beam port in the second measurement room. Small and constant long-term drifts are subtracted from the data, so that the intensity fluctuations shown in Fig. 2 are due probably to fast variations of the RF power provided to the pre-buncher, the buncher, and the main accelerating tube. The standard deviation of the intensity fluctuation is 0.25 % at the exit of the linac and it is 0.34 % in the second measurement room. These values are respectively one tenth of previous values measured before the remodeling. However, the intensity fluctuation is larger in the second measurement room than at the exit of the linac. It is considered that this increase is produced mainly by the energy fluctuation of the electron beam, because the energy dispersion is produced between two bending magnets in the beam line to bend the electron beam to the right by 90 degrees to the 2nd experimental room, as can be seen in Fig. 1. When the RF power changes, not only the beam intensity but also the beam energy changes. With BCM2 we can see the intensity change but not effects of the energy change, because there is no energy dispersion in the straight line. The beam transport line to the 2nd experimental room is designed to be achromatic, so that the energy dispersion is expected to be zero at BCM3. The energy dispersion in the horizontal direction is, however, non-zero between the two bending magnets comprising the achromatic bend and it probably leaks to BCM3 somewhat in the actual beam line. Then the tail of the transverse distribution of electrons is scraped off due to the energy fluctuation.

The stability of the electron beam is significantly increased and consequently the remodeling of the linac is successful. More detailed description of the upgrade of the L-band linac and evaluation of its performance will be published elsewhere [2].

DEVELPOMENT OF A STRONG FOCUS WIGGLER FOR FEL AND SASE

We have proposed and have been developing a novel wiggler named the Edge-Focus wiggler (EF-wiggler) for FEL and SASE [3]. First we fabricated a mode wiggler with five periods to demonstrate its performance, details of which will be published elsewhere [4]. As an application of the EF wiggler, we have fabricated a strong focus wiggler based on the EF wiggler for FEL and SASE experiments at ISIR, Osaka University. The main parameters of the SF wiggler are listed in Table 2. The period length is 6 cm and the number of periods is 32, which are the same with the conventional wiggler previously used. We have adopted a FODO structure

Table 2: Main Specifications of the SF Wiggler

Dimensions of permanent magnet blocks	90×20×15 mm^3
Permanent magnet and its surface coating	Nd-Fe-B, TiN
Period length and the number of periods	60 mm, 32 periods
Total length	1.938 m
Peak magnetic field	0.39 T (gap 30 mm)
Number of FODO cells and the cell length	4 cells, 0.48 m
Field gradient and the edge angle	3.2 T/m, 5 deg.

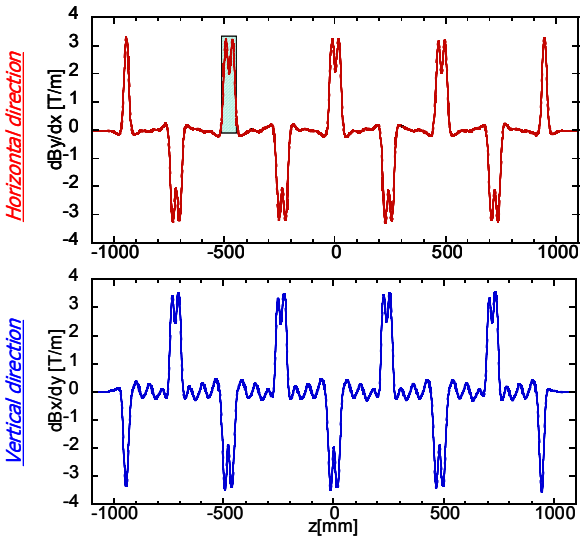

Figure 3: Magnetic field gradients of the strong focus wiggler in the horizontal and the vertical directions.

consisting of 4 cells for focusing the electron beam in the wiggler. A focusing unit or defocusing unit is one period EF wiggler with the edge angle of ±5 degrees and a drift space is filled with three periods of the normal wiggler, so that three normal wiggler periods are sandwiched between a focus unit and a defocus unit. The field gradient is derived from the magnetic field measured along the longitudinal axis at several transverse positions in the wiggler. Fig. 3 shows field gradients in the horizontal and the vertical directions as a function of the longitudinal position in the wiggler. The peak intensities of the field gradient vary randomly by approximately 1 % in each direction. The field gradient is, on the other hand, systematically and approximately 5 % higher in the vertical direction than in the horizontal direction. The measured field gradient in the horizontal direction agrees with the calculated one within 1 % accuracy. It seems that there are small orientation errors in the Hole probes and their translation stage, so that the field gradient derived from the measured magnetic field shows systematic

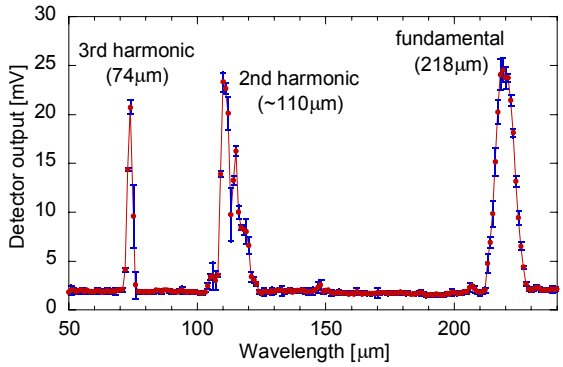

Figure 4: Wavelength spectrum of SASE.

deformation. One of these effects is corrected for the field gradient in the horizontal direction shown in Fig. 3, but the oscillation of the field gradient in the vertical direction remains in the regions where no field gradient is expected. More detailed analysis is still in progress to correct the measured magnetic field by taking effects of all the orientation errors into account.

SASE EXPERIMENTS

We have begun SASE experiments with the SF wiggler. The EF wiggler can focus the electron beam strongly along the whole wiggler length only when the betatron functions and its derivatives both in horizontal and vertical directions in the beam line are smoothly connected at the entrance of the wiggler to those optimised values in the wiggler. This is made by measuring the Twiss parameters in the beam transport line for FEL and then by setting them to the optimised values at the entrance of the EF wiggler. Although these procedures are not completely finished, we have measured the energy spectrum of SASE as shown in Fig. 4, in which not only the fundamental peak of SASE at 218 μm but also the second harmonic and the third harmonic peaks due to the non-linear generation of SASE show up. The experiments with the SF wiggler are in progress.

ACKNOWLEDGEMENTS

The development of the EF wiggler and the SF wiggler is being conducted with Prof. S. Yamamoto and his group in support of the KEK cooperative research and development program.

REFERENCES

[1] G. Isoyama, Y. Honda, S. Kashiwagi, R. Kato, T. Kozawa, S. Seki, S. Suemine, S. Tagawa, T. Yamamoto, Y. Yoshida, Proc. of APAC '04.
[2] R. Kato, et al., to be submitted to NIM.
[3] G. Isoyama, M. Fujimoto, R. Kato, S. Yamamoto, K. Tsuchiya, Nucl. Instr. Meth. A507 (2003) 234-237.
[4] S. Kashiwagi, et al., to be submitted to NIM.